Bursting of Underwater Oil Drops

Varun Kulkarni, Venkata Yashasvi Lolla, Suhas Tamvada, and Sushant Anand*
Department of Mechanical and Industrial Engineering, University of Illinois, Chicago, Illinois 60607, USA

(Received 24 October 2023; accepted 24 May 2024; published 18 July 2024)

For decades, two main facets of underwater oil spills have been explored extensively—the rise of oil drops and resulting evolution of the oil slick at the air-water interface. We report on the bursting of rising oil drops at an air–liquid interface which precedes slick formation and reveal a counterintuitive *bulge* reversal that releases a daughter oil droplet inside the bulk as opposed to upward-shooting jets observed in bursting air bubbles. By unraveling the underlying physics we show that daughter droplet size and bulk liquid properties are correlated and their formation can be suppressed by an increase in the bulk viscosity.

DOI: 10.1103/PhysRevLett.133.034004

Oil-water interactions lie at the root of diverse beneficial applications, such as drug delivery [1], oil recovery [2], food emulsions [3], and material synthesis [4], but they are also a subject of immense environmental concern due to oil and spills [5,6]. While oil in oceans may date back to ancient times [7], our excessive reliance on oil and its transportation has increased their prevalence, worsening their environmental and economic impact [8,9]. Consequently, for decades researchers worldwide have focused on studying major aspects of the oil spill process: rising of oil droplets through water [10], oil drops gently falling onto a liquid bath [6,11,12], and oil film spreading on an air-water interface [6,13]. Although the coalescence at a liquid-liquid interface [14,15] has been investigated, surprisingly, how an oil drop rising within the ocean transitions to an oil slick (forming a three-phase contact line) after breaching the air-water interface remains unexplored. This scenario bears similarities to the extensively studied phenomenon of bubbles bursting at an air-water [16–18] and air-oil-water interface [19]. For instance, in both cases, buoyancy plays a pivotal role in draining the liquid around the air bubble or oil drop. In air bubbles, the thin liquid film retracts in air [17], while for oil drops, the film retracts in the air on one side and over the oil drop's surface on the other [20], introducing significant viscosity effects in the latter case. Upon film retraction, bursting air bubbles produce jets which release droplets upward into the air. However, it is unclear whether the same can occur when oil drops burst upon breaching an air-liquid interface.

In this Letter, we study the bursting process of oil drops at an air-liquid interface. We show that an oil drop does not always directly transition to forming an oil slick but can also form daughter droplets within the bulk liquid through a fascinating bulge reversal. Such a *reversal* (oriented parallel to gravity) is contrary to vertically rising jets (oriented antiparallel to gravity) generated by bursting air bubbles [17] or liquid cylinders in falling drops [11] impacting liquids. The daughter droplet so released, cascades, forming a smaller droplet each time until the smallest droplet bursts to merge completely with the overlaying oil slick. Although similar cascades have been reported for *falling* drops [6,12,14,21,22] they are known to experience drop distortion which releases a daughter droplet, $\mathcal{O}(100\ \mu\text{m})$ only upward unlike *rising* drops which we show can exhibit both downward drop distortion in the case of drops and jetting upward for air bubbles, producing $\mathcal{O}(100\ \mu\text{m})$ daughter droplets (see Supplemental Material [23] Secs. S1 and S2 for a detailed literature review and details of prevalent mechanisms). Using experimental and theoretical analysis, we establish the conditions for bulge reversal and downward droplet formation, demonstrate its control by merely changing the bulk viscosity, and conclude by determining the scaling for daughter droplet sizes.

To explore the dynamics of drop bursting, we constructed an experimental setup [see Figs. 1(a) and 1(c)] in which air bubbles or parent (p) oil drops of radius R_p of different sizes emerging from a nozzle gently impact the bulk (b) fluid-air (a) interface (< 1 cm/s). We used hexadecane, pentane, and silicone oil as drops and glycerol-water mixtures 0–80 wt. % varied in increments of 10 wt. % as bulk fluids which have higher density, ρ_b (in kg/m^3) than the oil drops, (ρ_p in kg/m^3) with a density ratio, $\rho_r = \rho_b/\rho_p > 1$. The dynamic viscosity, μ_p was in the range of 0.24 to 3.005 mPas while μ_b varied between 1 to 60 mPas. Higher oil (drop) viscosity would dampen the capillary waves at their incipience and hence completely eliminate daughter droplet generation, therefore, in this work we consider any wave damping only through a change in bulk viscosity. For the oils, spreading coefficient, $S = \sigma_{pa} - \sigma_{ba} - \sigma_{pb}$ (in N/m) with respect to water [35] where, σ_{pb} represents the interfacial tension between the parent oil drop and bulk liquid, σ_{pa} is the surface tension of oil and σ_{ba} is the surface tension of bulk liquid, all expressed in N/m. $S > 0$ corresponds to oil spreading on the bulk forming a film (e.g., silicone oil and pentane),

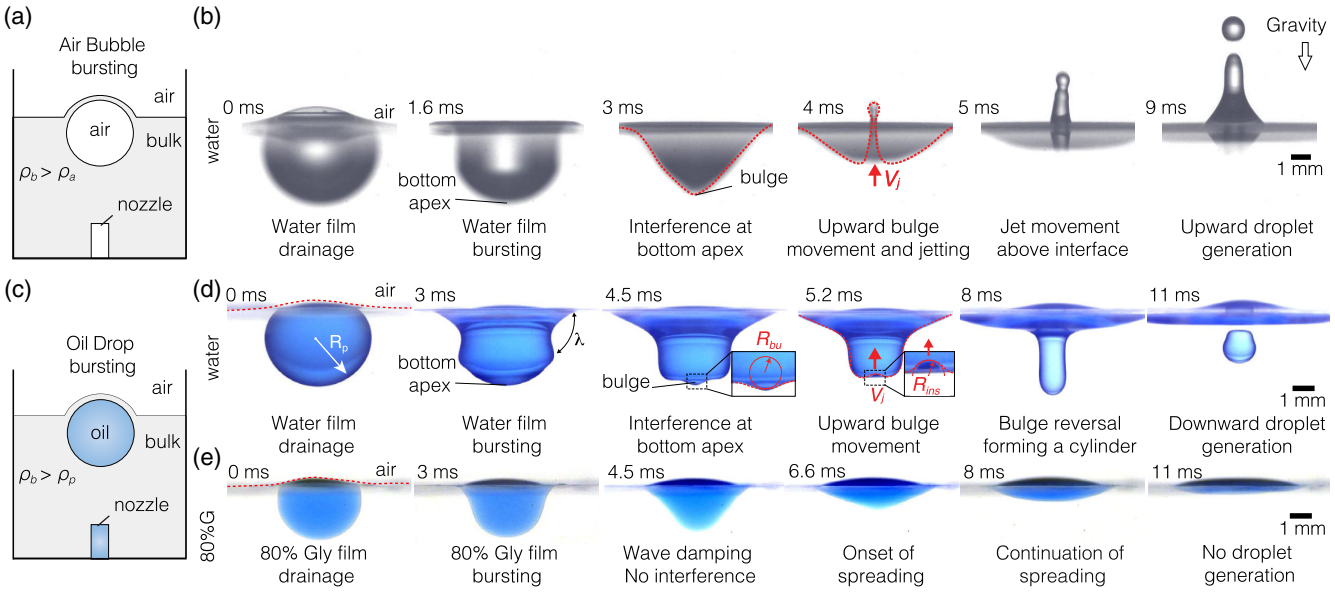

FIG. 1. (a) Schematic depicting gently impacting air bubbles at a liquid-air interface (b) Image sequence of a bursting air bubble showing *upward* jetting with bulge moving at velocity, V_j at $t = 4$ ms. (c) Schematic depicting gently impacting oil drops at a liquid-air interface. Image sequence of a hexadecane drop after bursting at (d) water-air interface leading to bulge reversal and generation of a downward daughter droplet ($t = 11$ ms) with bulge moving at velocity, V_j at $t = 5.2$ ms and, (e) 80 wt. % glycerol-air interface leading to complete emergence without bulge reversal and upward daughter droplet formation.

as opposed to $S < 0$, where the oil is nonspreading, taking a lenticular shape on the bulk (e.g., hexadecane) [6]. The oils were chosen such that they have similar physical properties [36,37] to light crude oils and petroleum hydrocarbons found in oil spills. We combine these quantities to concisely describe our results in terms of two dimensionless groups, namely the Ohnesorge number, $\mathrm{Oh}_b = \mu_b/\sqrt{\rho_b \sigma_{pb} R_p}$ of the bulk fluid and viscosity ratio of the bulk fluid to drop, $\mu_r = \mu_b/\mu_p$. Values for fluid properties, dimensionless groups and setup details are presented in Supplemental Material [23] Sec. S3. For visualization, the oil drops were stained using an oil-soluble dye—Sudan Blue II—to easily differentiate them from the bulk liquid which was not dyed for any case (oil drops or air bubbles).

Figure 1(b) shows evolution of an air bubble bursting at an air-water interface. Following thin bulk liquid film rupture, capillary waves propagate downward, leading to the formation of a highly curved region at its apex ($t = 3$ ms). The momentum of this region produces an upward liquid jet ($t = 4$ ms), which then pinches off to release daughter drops in the air ($t = 5$ and 9 ms). In contrast, the temporal evolution of an oil drop bursting at the air-water interface is shown in Fig. 1(d). Here, on rupture of the liquid film, [see Fig. 2(a), Video S1 and S2, Sec. S6] capillary waves rapidly descend straddling the oil-water interface while continuously being attenuated by viscosity of the drop and the bulk (see Video S1, Sec. S6). Upon reaching the bottom apex of the drop they constructively interfere to form a *bulge* (bu) [17] ($t = 4.5$ ms) of radius of curvature, R_{bu}.

The bulge inverts due to an interfacial stress, $\sim\sigma_{pb}/R_{\mathrm{bu}}$ forming a protrusion inside (ins) of a lower radius of curvature, R_{ins} (at $t = 5.2$ ms) and higher interfacial stress, $\sim\sigma_{pb}/R_{\mathrm{ins}}$ before finally undergoing another reversal which pulls the drop downward with it, parallel to gravity. The downward moving (deformed) drop takes a cylindrical liquid shape ($t = 8$ ms) that ultimately pinches off, leaving behind a daughter droplet ($t = 11$ ms) few 100 μm in size, inside the water bath. The observation of *bulge reversal* in systems comprising oil drops rupturing at an air-water interface is independent of S and has been unreported so far. To examine the controllability of this behavior, we substitute the water bath with glycerol-water solutions possessing higher viscosity in which capillary waves

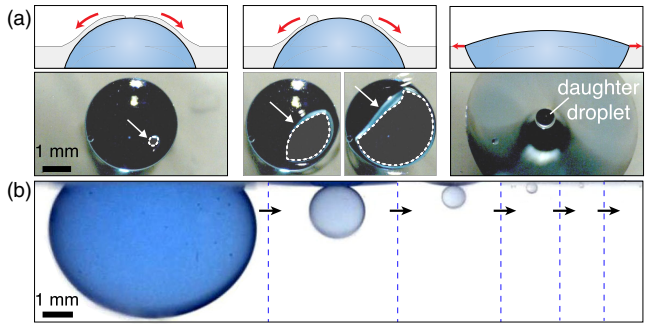

FIG. 2. (a) Schematic (above) and top view (below) showing—hole formation, hole expansion, and spreading of drop with a submerged daughter droplet. (b) Bursting cascade forming daughter droplets leading to complete emergence.

are strongly dissipated (typically > 50 wt. % glycerol) thereby precluding daughter droplet generation [Fig. 1(e), Video S1, Sec. S6].

When bulge reversal produces a daughter droplet, a cascade of bursting events is triggered which produces smaller sized daughter droplets until complete emergence (not coalescence since drop and bulk phases are different) occurs with oil floating atop water [Fig. 2(b), also see Video S3, Sec. S6]. From a practical standpoint, it indicates that drops bursting at an water-air interface from underwater oil spills can disperse daughter droplets deep inside the oceans. Furthermore, marine biosurfactants within the oceans [38,39] can arrest daughter droplet generation cascade and prolong oil droplet lifetimes, aspects which can be explored in future studies. Finally, we are concerned with drop distortion which leads to daughter droplets of size, $\mathcal{O}(100\ \mu\text{m})$ unlike previously reported [24] bubbles of secondary jets which are produced downward but much smaller in size $\mathcal{O}(4\text{–}5\ \mu\text{m})$.

To understand in detail why the bulge reverses and distorts the drop downward the we closely examine the bulge movement after it forms. So far we have broadly outlined interfacial tension stress as being important to bulge reversal. However, the associated interfacial energy opposes the kinetic energy of the bulge moving with a velocity V_j immediately after its reversal [see Fig. 1(d), 5.2 ms] similar to the description for bursting air bubbles [17] shown at a slightly later instant in Fig. 1(b), 4 ms after the bulge has assumed the form of a discernible upward jet. V_j, strictly speaking, is a function of μ_b, μ_p, σ_{pb}, R_p with the explicit dependence on these variables not considered for simplicity. The combined effect of these quantities [18,25] on V_j implies that for jets emanating from air bubbles its value is higher than for oil drops (see Supplemental Material [23] Sec. S2 for experimental values). This is because the bulge is slowed down by both the viscosity of the oil drop and the bulk. Specifically, in the case of oil drops, a comparatively high interfacial tension stress develops at its tip (of radius R_{ins}) which carries a lower kinetic energy and forces it to reverse direction parallel to gravity, pinching off a daughter drop. Conversely, for an air bubble, the surface tension stress that develops at its tip (of radius R_{ins}) may be similar but possesses a higher kinetic energy which forces it to continue its movement vertically upward [17,26].

While the above is necessary for bulge reversal an overarching condition also needs to be met. This requires the excess kinetic energy (per unit volume) of the interfering waves, $\sim\rho_b V_j^2/2$ contained in the bulge when it moves upward at velocity V_j [see Fig. 1(b) at $t = 4$ ms and Fig. 1(d) at $t = 5.2$ ms] to be less than the gravitational energy (per unit volume), $(\rho_b - \rho_p)gR_p$ (accounting for buoyancy). With these considerations the condition for bulge reversal in dimensionless terms finally takes the form, $\rho_r(\rho_r - 1)^{-1}\text{Fr}^2 < 2$ where, $\text{Fr} = \text{V}_j/\sqrt{gR_p}$ is the

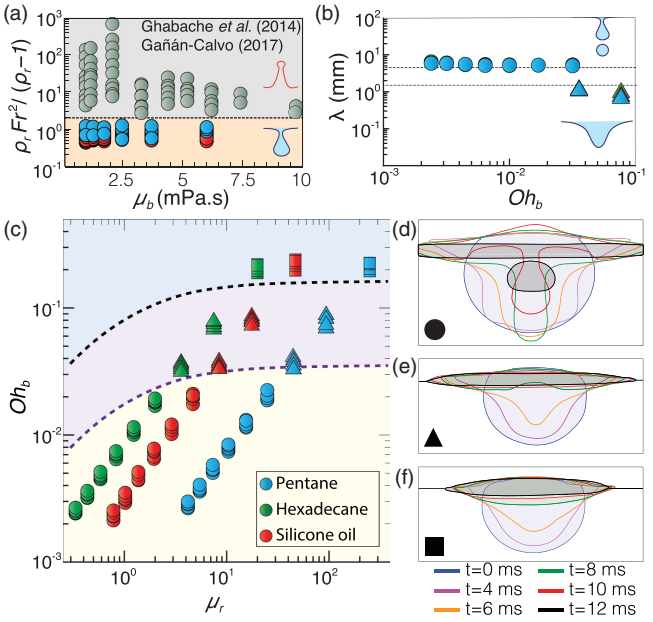

FIG. 3. (a) Criterion for reverse (present study) and upward bulge movement [17,26]. (b) Wavelength of waves for bulge reversal with droplet generation or partial (filled circles) and delayed emergence (filled triangles). (c) Different regimes: bulge reversal with daughter droplet generation, partial emergence (filled circles), bulge reversal with no daughter droplet generation, delayed emergence (filled triangles) and complete emergence (filled squares) as a function of μ_r and Oh_b. Drop profiles at different time instants for (d) partial, (e) delayed, and (f) complete emergence.

Froude number and g is the acceleration due to gravity [shown in Fig. 3(a)]. The criterion developed here compares well with our experimental data and previous work [17,26].

Having discussed the condition for *bulge reversal* we investigate how the strength of capillary waves that generate it, may or may not produce daughter droplets with *partial emergence* above the water-air interface of the remaining oil drop. To establish boundary of when this would happen we analyze the dynamics of capillary waves produced and their travel along the oil-bulk liquid interface. A typical wave is represented by its amplitude, ξ_0, complex frequency (with real, re and imaginary, im parts), $\omega(= \omega_{\text{re}} + i\omega_{\text{im}})$ and wave number, k $(= 2\pi/\lambda$, where λ is the wavelength) enabling depiction by the form $\xi = \xi_0 e^{\omega t + ikx}$ where t and x represent the time and spatial coordinate respectively. When $\omega_{\text{im}} \neq 0$, we observe traveling waves that elongate the drop and characteristic of *bulge reversal*. To clearly identify when this leads to daughter droplet generation we henceforth use the term *partial emergence* and, when it does not, we use *delayed emergence*. For $\omega_{\text{im}} = 0$, monotonically decaying standing waves are observed without any drop elongation and the drop emerges above the air-bulk fluid interface completely, referred to as *complete emergence*. The real part of the

complex frequency, ω_{re} is representative of the decay (or dissipation) rate of the waves. A dispersion relation for capillary waves which includes appropriate corrections for two superposed fluids [27] can be written in these terms as,

$$\omega = -Ak^2 \pm \sqrt{A^2k^4 - Bk^3 - Ck}. \tag{1}$$

In the above, the first term, $-Ak^2$ represents ω_{re} or dissipation rate, $\mathcal{D}$ and the second term $\sqrt{A^2k^4 - Bk^3 - Ck}$ represents ω_{im} which relates to wave velocity as, $v = \omega_{im}/k$. Here, $A = 2(\mu_b/\rho_b)(1+\mu_r)(1+\rho_r) - 1$, $B = 2\sigma_{pb}/\rho_p(1+\rho_r) - 1$, $C = g(\rho_r - 1)/(\rho_r + 1)$. Detailed algebra leading to Eq. (1) appears in Supplemental Material [23], Sec. S4.

To demarcate *partial or delayed emergence* from *complete emergence* we inspect the second term inside the square root, $A^2k^4 - Bk^3 - Ck$ in Eq. (1). When this term is negative, $\omega_{im} \neq 0$, the waves travel with v and we observe *partial* or *delayed emergence*. Conversely, if it is positive, the waves decay immediately leading to *complete emergence*. Here, the term A^2k^4 accounts for the slowing down of the waves due to viscosity [28] of oil drop and bulk fluid. Accordingly, the criterion for *partial or delayed emergence* can now be written as $A^2k^4 - Bk^3 - Ck < 0$. Gravity effect though important for bulge reversal does not influence the wavelength since the parent drop Bond number, $Bo_p = (\rho_b - \rho_p)R_p^2 g/\sigma_{pb} < 1$ (see Supplemental Material [23] Sec. S4) which implies $C = 0$ and $A < \sqrt{B/k}$. Substituting for A and B in terms of Oh_b, μ_r, ρ_r, kR_p and using the relation, $\mathrm{Oh}_b = (\mu_r/\sqrt{\rho_r})\mathrm{Oh}_p$ we obtain,

$$\mathrm{Oh}_b < \sqrt{\frac{1+\rho_r}{4kR_p\rho_r}}\frac{\mu_r}{1+\mu_r}. \tag{2}$$

Since $\rho_r \approx 1.55$ for our test conditions (see Supplemental Material [23] Secs. S2 and S4), the prefactor to $\mu_r/(1+\mu_r)$ in Eq. (2) reduces to $\sqrt{0.4/kR_p}$. To find k, we experimentally measure λ, the distance between two successive crests of the traveling wave train [see Fig. 1(d), $t = 3$ ms, Supplemental Material [23] Sec. S4] near the base. We find $\lambda = \text{constant} = 1.34$ mm across a range of Oh_b near the transition boundary. kR_p is therefore around 12.4 for $R_p \approx 2.65$ mm [see Fig. 3(b)] giving a value 0.18 for the prefactor. This boundary is shown by black dotted (upper) curve in Fig. 3(c).

Next, we establish the boundary between *partial* and *delayed emergence* [see Fig. 3(c), purple dotted (lower) curve] once Eq. (2) is satisfied. Prior studies [16,17] on bubble bursting state that for bulge movement without reversal or, jetting to occur, the waves should not dissipate in amplitude completely before reaching the bottom apex, i.e., $\mathcal{D}t_{base} < 1$ [12,16,21] where, t_{base} is the time the waves take to reach the bottom apex. The length (L) the wave needs to travel to reach the base is $(\pi/2)R_p$ which can be used to calculate t_{base} as L/v. We use the same for downward traveling waves due to their generality and from Eq. (1) deduce, $\mathcal{D} = Ak^2$ and $\omega_{im} = \sqrt{A^2k^4 + Bk^3 + Ck}$. After substituting for A, B, and C and neglecting gravity for small $Bo_p < 1$, we obtain the following criterion,

$$\mathrm{Oh}_b < \sqrt{\frac{1+\rho_r}{4kR_p(\pi^2k^2R_p^2+1)\rho_r}}\frac{\mu_r}{1+\mu_r}. \tag{3}$$

For the tested oils $\rho_r \approx 1.55$ and at transition to *partial emergence* we found the experimental value of $\lambda = 4.6$ mm measured in a similar manner (see Supplemental Material [23] Sec. S4) as before we get values of $kR_p \approx 3.7$ for $R_p \approx 2.65$ mm [see Fig. 3(b), triangles]. This yields an inequality like the previous criterion but with a constant prefactor of 0.028 (for more details see Supplemental Material [23] Secs. S3 and S4) where the theoretical regime boundary is represented by the purple dashed line in Fig. 3(c). To validate Eq. (3), we compare it with the case of an air bubble bursting in water using, $\mu_r \gg 1$, $\rho_r \gg 1$, and $\pi k^2R_p^2 \gg 1$. Since the wavelength is small due to the low viscosity of water Eq. (3) now simplifies to $2\pi\mathrm{Oh}_b(kR_p)^{3/2} < 1$ recovering previous results exactly [12,21].

Time resolved experimental outlines for different regimes are shown in Figs. 3(d)–3(f) for the three oils tested. The profiles in Fig. 3(e) (filled triangles) and Fig. 3(f) (filled squares) do not produce droplets; however, we can see a relatively sharper traveling wave at $t = 6$ ms (orange line) Fig. 3(e) in comparison to the one for the standing decaying wave in Fig. 3(f) which served to distinguish visually *partial or delayed* from *complete emergence*. Note that we did not observe satellite droplet formation and our results directly relate to oil spills in water bodies which often have varying bulk viscosities due to their composition, salinity, and temperature [40]. Further, given the broad nature of the derived criteria 2 and 3, we envision these to be applicable to coalescence at liquid-liquid interfaces too [29].

A salient aspect of *partial emergence* is generation of a daughter droplet of size, R_d whose scaling we determine next. Figure 4(a) schematically shows the deformed drop just before and after the pinch-off. After the waves interfere at the base at $t = t_0$ a cylindrical entity of diameter, d, and length, l is formed that moves downward with an average velocity, $V_{po} = l/t_{po}$ and thins continuously as shown at $t = t_1$, eventually pinching off in time $t = t_{po} = \sqrt{\rho_p R_p^3/\sigma_{pb}}$. The thinning initially is a result of downward movement of the cylinder and is accompanied by horizontal spreading above the interface such that the two motions compete against each other forming a neck with the final

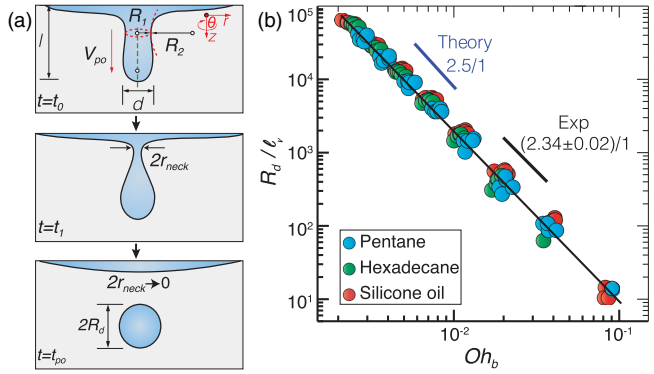

FIG. 4. (a) Schematic showing drop profile at three time instances, t_0, when a cylindrical entity is formed, t_1, during thinning and, t_{po} when a daughter droplet is pinched off. (b) Scaling for the dimensionless daughter droplet radius, R_d/ℓ_v with Oh_b.

pinch-off being capillary driven [11,12]. The pressure difference inside and outside the neck, $p_{\mathrm{in}} - p_{\mathrm{out}} = \Delta p_{\mathrm{neck}}$ during thinning equals $-r_{\mathrm{neck}}^{-1}\sigma_{pb}$ as $r_{\mathrm{neck}} \to 0$ and $R_1, R_2 \gg r_{\mathrm{neck}}$ pushing away the oil from the neck ultimately generating a daughter droplet of volume, $(4/3)\pi R_d^3$ which equals the volume of cylindrical entity, $\pi d^2 l/4$ before pinch-off.

The scaling law for R_d hence can be ascertained once the scaling for l and d is known. To begin we assume the flow inside the cylindrical entity as near inviscid while that outside (bulk) to be viscous since $\mu_r > 1$. At the moving cylindrical liquid front the viscous, $F_v \sim (\mu_b V_{po}/R_p)ld$ and capillary force $F_c \sim \sigma_{pb} d$ are balanced yielding, $l \sim (\sigma_{pb} R_p/\mu_b)V_{po}^{-1}$. Simplifying further we get, $l^2 \sim (\rho_r/\mathrm{Oh}_b)^{1/2} R_p^2$. For, $\rho_r \approx 1.3$ and using the scale $\ell_v = \mu_b^2/\rho_b\sigma_{pb}$ [17] for making l dimensionless, since the bulge leading to formation of daughter droplet is analogous to bubble bursting we eventually obtain, $l/\ell_v \sim \mathrm{Oh}_b^{-5/2}$. As the energy of waves at the bottom apex decreases with an increase in bulk viscosity, $l \sim d$ and confirmed *a posteriori* by our experimental data (see Supplemental Material [23] Sec. S5) which show exponents of -2.23 and -2.25 for l and d respectively. The scaling for R_d using the previously stated mass conservation results in, $R_d/\ell_v \sim \mathrm{Oh}_b^{-5/2}$. The scaling exponent of $-5/2$ shown in Fig. 4(b) is within 7% of -2.34 obtained from fitting. The close agreement between theory and experiments despite assuming inviscid flow inside the drop shows that viscous effects arising from the drop may be insignificant for our experimental conditions.

To summarize, this work shows that the bursting of a rising oil droplet at a liquid-air interface can lead to previously unreported bulge reversal and daughter droplet formation which are distinct from observations on coalescence of oil drops gently falling on an air-liquid interface. We delineate the different outcomes in a regime map based on μ_r and Oh_b alone. Most studies heretofore have focused on oil slick formation on the interface however droplet generation under it suggests a new pathway for oil spill proliferation which can adversely affect aquatic life. Moreover, presence of surfactants can arrest daughter droplet cascade ensuring that the oil droplets remain inside the bulk for long periods. In addition to guiding oil spill remediation, our results could potentially be beneficial to numerous fields where oil-water interactions are important, these include oil recovery, drug delivery, food, and cosmetics.

Financial support by National Science Foundation EAGER Grant No. 2028571, UIC College of Engineering and Society in Science, Branco Weiss Fellowship is gratefully acknowledged.

*Corresponding author: sushant@uic.edu

[1] C.-X. Zhao, Adv. Drug Delivery Rev. **65**, 1420 (2013).
[2] L. Wang, Y. Tian, X. Yu, C. Wang, B. Yao, S. Wang, P. Winterfeld, X. Wang, Z. Yang, Y. Wang, and J. Cui, Fuel **210**, 425 (2017).
[3] D. G. Dalgleish, Food Hydrocolloids **20**, 415 (2006).
[4] L. D. Zarzar, V. Sresht, E. M. Sletten, J. A. Kalow, D. Blankschtein, and T. M. Swager, Nature (London) **518**, 520 (2015).
[5] C. H. Peterson, S. D. Rice, J. W. Short, D. Esler, J. L. Bodkin, B. E. Ballachey, and D. B. Irons, Science **302**, 2082 (2003).
[6] V. Kulkarni, V. Y. Lolla, S. R. Tamvada, N. Shirdade, and S. Anand, J. Colloid Interface Sci. **586**, 257 (2021).
[7] K. A. Campbell, J. D. Farmer, and D. D. Marais, Geofluids **2**, 63 (2002).
[8] A. Jernelöv, Ambio **39**, 353 (2010).
[9] P. S. Hill, A. Khelifa, and K. Lee, Spill Sci. Technol. Bull. **8**, 73 (2002).
[10] C. Albert, J. Kromer, A. M. Robertson, and D. Bothe, J. Fluid Mech. **778**, 485 (2015).
[11] T. Dong and P. Angeli, Phys. Rev. Lett. **131**, 104001 (2023).
[12] F. Blanchette and T. P. Bigioni, Nat. Phys. **2**, 254 (2006).
[13] S. L. Cormier, J. D. McGraw, T. Salez, E. Raphaël, and K. Dalnoki-Veress, Phys. Rev. Lett. **109**, 154501 (2012).
[14] G. E. Charles and S. G. Mason, J. Colloid Sci. **15**, 105 (1960).
[15] Z. Mohamed-Kassim and E. K. Longmire, Phys. Fluids **16**, 2170 (2004).
[16] J. S. Lee, B. M. Weon, S. J. Park, J. H. Je, K. Fezzaa, and W.-K. Lee, Nat. Commun. **2**, 367 (2011).
[17] A. M. Gañán-Calvo, Phys. Rev. Lett. **119**, 204502 (2017).
[18] A. M. Gañán-Calvo, Phys. Rev. Fluids **3**, 091601(R) (2018).
[19] B. Ji, Z. Yang, and J. Feng, Nat. Commun. **12**, 6305 (2021).
[20] V. Sanjay, U. Sen, P. Kant, and D. Lohse, J. Fluid Mech. **948**, A14 (2022).
[21] F. Blanchette and T. P. Bigioni, J. Fluid Mech. **620**, 333 (2009).

[22] S. T. Thoroddsen and K. Takehara, Phys. Fluids **12**, 1265 (2000).
[23] See Supplemental Material at http://link.aps.org/supplemental/10.1103/PhysRevLett.133.034004 for details of literature review, mechanisms, setup, fluid properties, theory and includes Refs. [6,12,14–19,21,22,24–34].
[24] F. MacIntyre, J. Geophys. Res. **77**, 5211 (1972).
[25] A. Berny, L. Deike, T. Séon, and S. Popinet, Phys. Rev. Fluids **5**, 033605 (2020).
[26] E. Ghabache, A. Antkowiak, C. Josserand, and T. Séon, Phys. Fluids **26** (2014).
[27] D. Joseph, J. Wang, and T. Funada, *Potential Flows of Viscous and Viscoelastic Liquids* (Cambridge University Press, Cambridge, England, 2007).
[28] J. C. Padrino and D. D. Joseph, Phys. Fluids **19** (2007).
[29] H. P. Kavehpour, Annu. Rev. Fluid Mech. **47**, 245 (2015).
[30] T. Gilet, K. Mulleners, J. P. Lecomte, N. Vandewalle, and S. Dorbolo, Phys. Rev. E **75**, 036303 (2007).
[31] B. Ray, G. Biswas, and A. Sharma, J. Fluid Mech. **655**, 72 (2010).
[32] J. B. Segur and H. E. Oberstar, Ind. Eng. Chem. **43**, 2117 (1951).
[33] C. L. Yaws, *Yaws' Handbook of Physical Properties for Hydrocarbons and Chemicals* (Gulf Professional Publishing, Houston, 2015).
[34] S. Krishnan, E. J. Hopfinger, and B. A. Puthenveettil, J. Fluid Mech. **822**, 791 (2017).
[35] P.-G. Gennes, F. Brochard-Wyart, and D. Quéré, *Capillarity and Wetting Phenomena: Drops, Bubbles, Pearls, Waves* (Springer, New York, 2004).
[36] Karen Schou Pedersen, A. Fredenslund, P. L. Christensen, and P. Thomassen, Chem. Eng. Sci. **39**, 1011 (1984).
[37] Rafa Labedi, J. Pet. Sci. Eng. **8**, 221 (1992).
[38] N. M. Dannreuther, D. Halpern, J. Rullkötter, and D. Yoerger, Oceanography **34**, 192 (2021).
[39] S. K. Satpute, I. M. Banat, P. K. Dhakephalkar, A. G. Banpurkar, and B. A. Chopade, Biotechnol. Adv. **28**, 436 (2010).
[40] M. Jochum, B. P. Briegleb, G. Danabasoglu, W. G. Large, N. J. Norton, S. R. Jayne, M. H. Alford, and F. O. Bryan, J. Geophys. Res. Oceans **26**, 2833 (2008).